

Chromodomain Antagonists That Target the Polycomb-Group Methyllysine Reader Protein Chromobox Homolog 7 (CBX7)

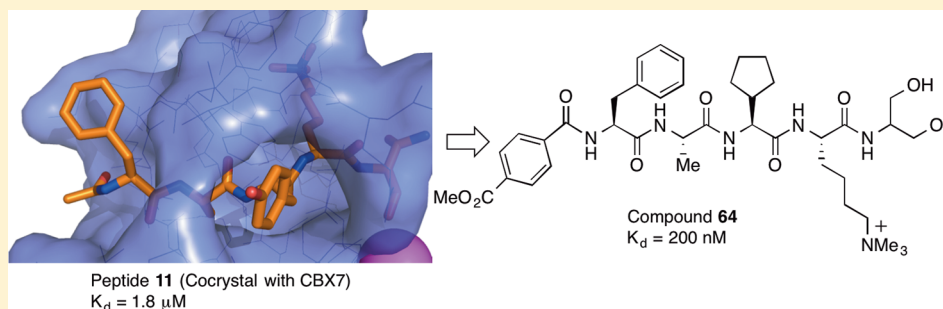
Chakravarthi Simhadri,^{†,‡} Kevin D. Daze,^{†,‡} Sarah F. Douglas,[†] Taylor T. H. Quon,[†] Amarjot Dev,[†] Michael C. Gignac,[†] Fangni Peng,[‡] Markus Heller,[§] Martin J. Boulanger,[‡] Jeremy E. Wulff,[†] and Fraser Hof^{*,†}

[†]Department of Chemistry, University of Victoria, P.O. Box 3065, Victoria, British Columbia, V8W 3V6, Canada

[‡]Department of Biochemistry and Microbiology, University of Victoria, P.O. Box 3065, Victoria, British Columbia, V8W 3V6, Canada

[§]Centre for Drug Research and Development, 2405 Wesbrook Mall, Vancouver, British Columbia, V6T 1Z3, Canada

S Supporting Information



ABSTRACT: We report here a peptide-driven approach to create first inhibitors of the chromobox homolog 7 (CBX7), a methyllysine reader protein. CBX7 uses its chromodomain to bind histone 3, lysine 27 trimethylated (H3K27me3), and this recognition event is implicated in silencing multiple tumor suppressors. Small trimethyllysine containing peptides were used as the basic scaffold from which potent ligands for disruption of CBX7-H3K27me3 complex were developed. Potency of ligands was determined by fluorescence polarization and/or isothermal titration calorimetry. Binding of one ligand was characterized in detail using 2D NMR and X-ray crystallography, revealing a structural motif unique among human CBX proteins. Inhibitors with a ~200 nM potency for CBX7 binding and 10-fold/400-fold selectivity over related CBX8/CBX1 proteins were identified. These are the first reported inhibitors of any chromodomain.

INTRODUCTION

A complex language of histone modifications is the basis for the epigenetic control of gene expression. In the metaphorical “histone code” there are “writer” and “eraser” proteins that add and remove modifications including methylation, acetylation, phosphorylation, ubiquitylation, SUMOylation, and others.¹ There are also “reader” proteins that recognize and bind to certain histone modifications, including acetyllysine, methyllysines, and methylarginines.^{2–4} Inhibitors of writer proteins like histone methyltransferases (HMTs) have entered the clinic,^{5–12} and inhibitors of histone deacetylase (HDAC) eraser proteins are approved and used clinically against multiple malignancies.^{13–15}

Very few reader proteins have yet been successfully targeted by small molecule agents. Acetyllysine marks are read by bromodomain-family proteins, and bromodomain inhibitors (which were the first inhibitors of any reader protein) have shown powerful and diverse biological activities.^{16–19} Methyllysine marks are read by a diverse set of hundreds of human proteins, with the major groups being the MBT, PHD, Tudor, PWWP, WDR, and chromodomain families.^{4,20,21} Many of

these proteins are predicted to be druggable.²² The first inhibitors of any methyllysine reader were reported to target a few similar members of a single family (the malignant brain tumour (MBT) proteins) and have moved quickly through subsequent rounds of optimization.^{23–27} As with bromodomain inhibitors, the first tool compound against an MBT domain has been demonstrated to have a potent influence on the biology of cancer cells.²⁸ Inhibitors of a PHD (plant homeodomain) methyllysine reader have also been recently disclosed.²⁹

We are primarily interested in developing tool compounds to probe the activities of protein chromodomains (“chromatin organization modifier” domains), which are a family of methyllysine readers generally associated with chromatin remodeling.^{30–32} Thirty-one human chromodomains exist,²⁰ and each is predicted to act as a modular unit for the recognition of a mono-, di-, or trimethyllysine modifications in different structural contexts. One major family of human chromodomains are the paralogs of the *Drosophila* protein

Received: September 25, 2013

Published: March 13, 2014

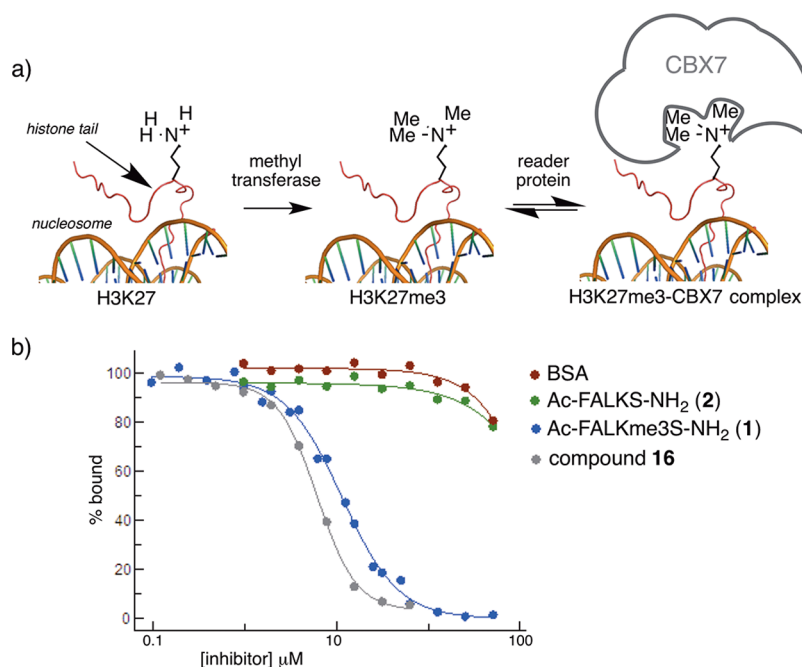


Figure 1. (a) The product of a methyltransferase (e.g., EZH2) acting on a histone lysine (H3K27) is a methylated residue (H3K27me3) that is recognized and bound by a reader protein (CBX7). (b) Competitive fluorescence polarization (FP) data can report on the disruption of the complex between recombinant CBX7 chromodomain and H3K27me3. Data shown arise from addition of compound 1 and compound 16 (as two examples of active compounds), compound 2, unmethylated control, or BSA (additional control) to a solution containing CBX7 chromodomain (8.68 μM) and FITC-H3K27me3 probe peptide (500 nM).

Polycomb, called chromobox homolog (CBX) proteins CBX2, CBX4, CBX6, CBX7, and CBX8.³¹ Polycomb group genes are transcriptional repressors that play essential roles in development, cancer progression, and stem cell maintenance.³³ Polycomb group proteins form multiprotein polycomb repressive complexes (PRC1/2), members of which are frequently dysregulated in metastatic cancers in which tumor suppressor genes are silenced and stemlike phenotypes are acquired.^{33–35} Gene suppression is initiated by the writer protein enhancer of zeste homolog 2 (EZH2) of PRC2, which trimethylates lysine 27 on histone H3 to create the mark H3K27me3. The resulting gene-specific trimethyl marks then provide the binding sites for the reader components of PRC1 (CBX proteins) which cause gene silencing and ultimately lead to stable DNA methylation. The five human paralogs CBX2, -4, -6, -7, and -8 participate in a modular way within different PRC1 complexes.^{36,37} Each recognizes and binds to H3K27me3 mark laid down by EZH2 using its chromodomain but has distinct genetic targets, overall domain structure, and functional outcomes.^{36,37} CBX7 is the best-studied of the Polycomb paralogs; it is a master controller that extends cellular lifespan, delays senescence, drives proliferation, and bestows pluripotency to adult and embryonic stem cells.^{38–40}

Polycomb group proteins have been highlighted as being important in different malignancies.⁴¹ Multiple lines of evidence suggest promise for CBX7 as a therapeutic target in certain forms of cancer. CBX7 expression is strongly proliferative in various stem cell and stemlike cancer cell lines.^{36,38–40,42–44} The depletion or knockdown of CBX7 in both androgen-dependent (AD) and androgen-independent (AI) prostate cancer cell lines induces a senescent phenotype with reduced cell proliferation by repression of the p16^{INK4a}/p14^{ARF} tumor suppressor locus.^{39,40} CBX7 expression in the prostate increases as AD prostate cancer progresses to AI status; in a panel of 27

diverse cancer cell lines, higher CBX7 expression was observed in two lines of aggressive, AI cells (PC3, DU145) than in the AD line LNCaP (very high CBX7 was also seen in metastatic lymphoma (K299) and glioblastoma (U87MG) lines).³⁹ CBX7 expression significantly increases in clinical samples of hormone-resistant prostate cancer relative to hormone-dependent prostate cancer⁴⁵ and was recently linked to poor prognosis in ovarian clear cell adenocarcinoma.⁴⁴ CBX7 also plays a central role in some blood malignancies. It initiates and accelerates lymphomagenesis and cooperates with Myc to generate aggressive lymphomas.⁴³ Overexpression of CBX7 in hematopoietic stem cells drives proliferation and genesis of T-cell leukemia (while its close relative CBX8 does not).⁴⁶ CBX7 is consistently shown to be strongly proliferative in androgen-independent prostate cancer cells, embryonic and adult stem cells, and hematopoiesis/lymphomagenesis.^{36,38–40,42,43,46} These cell types are linked by their stemlike gene regulation and phenotypes.

Epigenetic targets like the CBX proteins often have strongly tissue- and context-selective functions, and the literature on CBX7 outside of the prostate, embryonic, hematopoietic, or stem-cell contexts contains some results that give pause.^{33,47–51} But many such functional studies on CBX7 involve the knockout/knockdown of the whole, multidomain protein that do not predict the outcome of chemical chromodomain antagonism. Critically, multiple reports show that the proliferative/prosurvival functions of CBX7 depend narrowly on its H3K27me3 binding ability; when a single Kme3-binding residue in its chromodomain is mutated, CBX7-driven proliferation disappears.^{39,40,52} Accordingly, our goal is to create tool compounds that antagonize the chromodomain of CBX7 in order to test the antiproliferative potential of this novel epigenetic target.

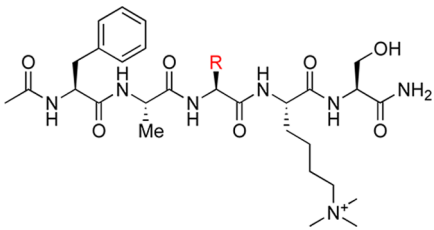
RESULTS AND DISCUSSION

Our early efforts at virtual screening failed to yield potent lead compounds against the CBX7 chromodomain. A high-throughput screen against the somewhat related chromodomain of CBX1 (HP1 β) was completed at the National Chemical Genomics Center but failed to produce tractable hits and was not published.⁵³ We were inspired to start on a search for peptidic antagonists of the CBX7 chromodomain by a report of the binding by CBX7 of a 25 amino acid long peptide sequence derived from the protein SETDB1, which was reported to have slightly higher in vitro affinity for CBX7 than the H3K27me3 sequence itself.³¹ We truncated the methylated SETDB1 sequence to arrive at a five amino acid long peptide (1) that demonstrated reasonable potency ($IC_{50} = 12 \mu M$) in a competitive fluorescence polarization (FP) assay for CBX7-H3K27me3 disruption (Figure 1). In a variety of in vitro and in vivo studies, CBX7 binding has been shown to depend strongly on the methylation of the lysine residue that binds in CBX7's aromatic cage motif made up of Phe5, Trp26, and Trp29 (numbering derived from the CBX7 chromodomain construct used in this study). This allowed us to demonstrate the specificity of the initial assay result by a control titration with the unmethylated analog (2), which showed no ability to displace H3K27me3 from CBX7 under the assay conditions (Figure 1). Thus, we used the small peptide (1) as a scaffold in order to establish structure–function relationships for CBX7 antagonism.

We built a simple, energy-minimized molecular model of the complex of CBX7 with Ac-FALKme3S-NH2 (1) starting with the published, NMR-derived structure 2L1B that shows CBX7 bound to its native histone tail partner, H3K27me3 (whose sequence at the trimethyllysine site is ...AARKme3S...).³¹ As in the native complex, the trimethyllysine residue makes multiple cation– π contacts to the aromatic cage motif of CBX7 (Phe5, Trp26, Trp29), and the adjacent (+1) Ser residue donates hydrogen bonds from side chain OH and backbone NH to the carboxylate side chain of Glu37. The molecular recognition requirements for the peptide's (–1) Leu residue were not immediately clear to us because, in addition to a hydrophobic contact with a well-ordered Val10 residue, it is close to the N-terminal CBX7 residues (Gly1/Glu2/Gln3) that are poorly ordered in the NMR structure. Thus, we first made a family of analogs of the peptide Ac-FALKme3S-NH2 that varied at the (–1) Leu position and tested them for their ability to disrupt the H3K27me3-CBX7 complex as indicated by fluorescence polarization assay (Table 1). A variety of hydrophobic and/or aromatic residues at this position provided strong (<10 μM) inhibitors. A preference for hydrophobic, β -branched residues can be clearly seen in the cases of compounds 3, 4, and 16. *n*-Alkyl inhibitors 6 and 7 are weak inhibitors, as is the overly bulky *tert*-butylglycine inhibitor 5. Aromatics are generally well tolerated.

We solved the X-ray structure of the complex of CBX7 with compound 11 to 1.54 Å resolution (Figure 2). The structure confirms the ligand binding pose predicted by modeling. The significant recognition elements are the trimethyllysine side chain participating in multiple cation– π interactions, extensive backbone-to-backbone β -sheet-like hydrogen bonding network between protein and ligand, the Ser(+1) residue of the ligand donating multiple H-bonds from side chain OH and backbone NH to Glu37 of the protein, and the Ala(–2) side chain of the ligand being nestled tightly into the small hydrophobic pocket

Table 1. H3K27me3-CBX7 Disruption by FALKme3S Analogs Bearing Leucine (–1) Replacements



Compound	R =	IC_{50} (μM) ^a
1	Leu	11 ± 0.4
3	Val	6.8 ± 0.2
4	Ile	5.7 ± 0.3
5	<i>t</i> Bu	67 ± 2
6	Nle	23 ± 2
7	Met	62 ± 5
8	Thr	35 ± 2
9	Lys	10.1 ± 0.5
10	Phe	10.3 ± 0.9
11	Tyr	6.2 ± 0.4
12	Trp	13 ± 0.3
13		11 ± 1
14		21 ± 1
15		11.2 ± 0.4
16		6.0 ± 0.2
17		8.8 ± 0.2

^a IC_{50} values were determined as the inhibitor concentration required for the half-dissociation of the complex between CBX7 and FITC-labeled H3K27me3. Data are mean values of two or three independent experimental trials. Errors reported are 95% confidence intervals.

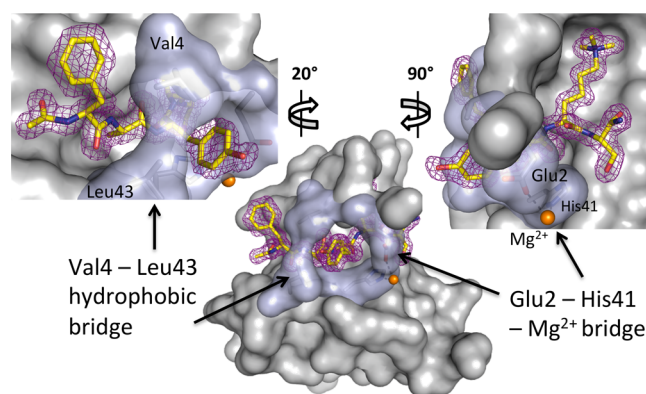


Figure 2. Cocrystal structure of CBX7 chromodomain bound to ligand 11 as determined by X-ray crystallography. CBX7 is shown as a gray solvent-accessible surface, and the ligand is shown as yellow sticks overlaid with the electron density contours (Coot). The hydrophobic clasp between Val4 and Leu43 is common to all chromodomains. The Mg^{2+} -mediated bridge between Glu2 and His41 appears to be unique to CBX7 among human CBX proteins.

of CBX7 that is largely responsible for its substrate-binding selectivity. The exposure of the (–1) substituent (in this ligand, Tyr) to solvent provides a good explanation for the tolerance of this position to different substitutions (Table 1). Unexpectedly, the X-ray structure also revealed a significantly more closed

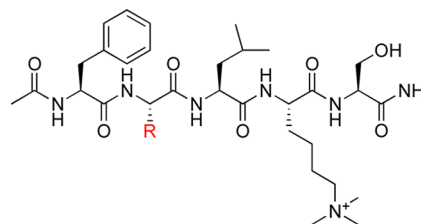
binding pocket than is depicted in the existing NMR structure of the CBX7-H3K27me3 complex.³¹ In addition to the “hydrophobic clasp,” which is a major side chain to side chain bridge that is formed by Val4/Leu43 in all Polycomb paralogs,³¹ the new structure revealed an unexpected metal-mediated bridge between Glu2 and His41 as an additional clasping motif that envelops the bound ligand. Neither the purification buffers nor the crystallization solutions contained any divalent metal, which was modeled as Mg²⁺. Our choice of Mg²⁺ for this model is supported indirectly by the facts that the tetrahedral coordination geometry⁵⁴ is that which would be observed for Mg²⁺, and that Mg²⁺ concentrations are high in chromatin. The biological relevance of the bound metal is unclear, but it is intriguing that CBX7 is unique among the eight human CBX proteins from both Polycomb and HP1 families in having a metal-binding His residue at position 41; all others have a Asn at this position and adopt a more open conformation (see Supporting Information).²² In solution, we found only small differences in ligand binding to CBX7 in the absence/presence of 2 mM MgCl₂ (data not shown), suggesting that this motif, while structurally unique, is not necessarily a significant determinant in ligand binding.

We carried out 2D NMR studies to confirm that the ligand-binding pose shown by X-ray also operates in solution. Titration of ligand **11** into an ¹⁵N-labeled sample of CBX7 was first followed by ¹H–¹⁵N HSQC. Mapping the binding-induced chemical shift changes for assigned backbone nitrogen resonances onto the structure of CBX7 provides a clear picture of the binding site that is consistent with X-ray data: Medium/large chemical shift perturbations occur for residues directly in contact with the Kme3 side chain (Gln3/Trp26/Trp29/Thr35) and with the contact partners for the inhibitor’s Phe and Tyr residues (His41/Leu43/Asp44; see Supporting Information). Further, the side chain methyl groups of Val4 and Leu43 are both predicted by models to be engaged with the faces of the ligand’s Tyr residue. Accordingly, ¹H–¹³C HSQC experiments showed that significant broadening and upfield chemical shift for these Val/Leu methyl groups occur upon addition of the peptide, adding specific support to this aspect of the protein–ligand complex shown in the crystal structure. With a good understanding of the binding mode in hand, we sought next to probe the structure–activity relationships in different subpockets of the binding site using a series of peptidic inhibitors.

The side chain of the ligand alanine (–2) position is buried in a small hydrophobic pocket of CBX7 that is an important determinant of protein–protein interaction specificity in the different natural complexes of chromodomains that have been studied. CBX7 (and all Polycomb homologues) have an exclusive preference for natural binding partners with an Ala residue at this position.³¹ We varied the parent FALKme3S structure by installation of a few small side chains (Table 2). We found that even an ethyl side chain (Abu) was too big to be accommodated in this pocket, and so Ala was retained at the (–2) position for all subsequent CBX7 ligands.

Both the backbone amide NH and the OH side chain of the serine (+1) residue donate hydrogen bonds to the side chain of Glu37, again forming one of the primary determinants for selection of binding partners by CBX7.³¹ The switch to D-Ser (**23**, Table 3) was tolerated without loss in affinity, suggesting some freedom of movement for the ligand in this pocket. The switch to C-terminal acid forms (Ac-FALKme3S-CO₂[–]) was detrimental to binding for peptides built from both D- and L-Ser stereoisomers. Other non-amino acid substitutions at the Ser

Table 2. H3K27me3-CBX7 Disruption by FALKme3S Analogs Bearing Alanine (–2) Replacements



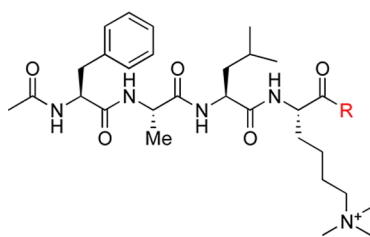
compd	R	IC ₅₀ (μM) ^a
1	Ala	11 ± 0.4
18	Abu	39 ± 3
19	Nle	120 ± 30
20	Ser	53 ± 3
21	Val	>500

^aIC₅₀ values were determined as the inhibitor concentration required for the half-dissociation of the complex between CBX7 and FITC-labeled H3K27me3. Data are mean values of two or three independent experimental trials. Errors reported are 95% confidence intervals.

position were made by preparing the C-terminal carboxy peptide Ac-FALKme3-CO₂[–] on 2-chlorotrityl resin, purification by HPLC, and subsequent coupling to a variety of different amines as shown in Scheme 1a. At this position, the installation of hydrophobic functionality significantly weakened binding (**26**, **27**, **35**), as did the inclusion of a variety of conformationally constrained bis-hydrogen bond donors **26**, **27**, **28**, and **29**. Happily, we found that simple H-bond-donating substituents, including an aminobenzimidazole (**30**), a propanediol (**33**), and a pendent ammonium group (**34**), served well in this region presumably because they can donate hydrogen bonds to Glu37 in a manner analogous to the ligand Ser residue that normally occupies this position.

The molecular recognition requirements of the extended β-groove region of CBX7, occupied by the Ac-F portion of Ac-FALKme3S-NH₂, were probed by two different families of inhibitors. The first group of Ac-FALKme3S-NH₂ analogs were made by replacing Phe with a natural or unnatural fragment (Table 4). Simple replacement of Phe with other aromatic amino acids gave peptides with only small changes in potency (Tyr, Trp, Phg). Installation of non amino acid groups at the N-terminus was achieved by preparing the peptide Fmoc-ALKme3S- on resin, with subsequent deprotection of the N-terminus and reaction with a variety of electrophiles and coupling partners (Scheme 1b). We found that the retention of a “backbone” C=O in this position, which is strongly ordered in the parent X-ray structure by accepting a hydrogen bond from the backbone NH of Val7, is critically important. Replacement of this C=O with a sulfonamide linkage (**48**, **49**) was detrimental, while the use of on-resin reductive aminations to produce benzylamine-type linkages (**52**, **53**) completely abrogated ligand binding. The potency of amide- and carbamate-type compounds that preserve this ligand C=O was generally good, with variations depending on the exact nature of aromatic substituent and linker directed into the β-groove.

A second group of analogs that probe this binding site were prepared by leaving the Phe residue in place and installing additional fragments at the N-terminus of the ligand peptide (Scheme 1c, Table 5). N-terminal benzamides and phenylacetamides of FALKme3S are generally potent inhibitors (**54**,

Table 3. H3K27me3-CBX7 Disruption by FALKme3S Analogs Bearing Serine (+1) Replacements

Compound	R =	IC ₅₀ (μM) ^a
1	L-Ser-NH ₂	11 ± 0.4
22	L-Ser-OH	27 ± 1
23	D-Ser-NH ₂	9 ± 1
24	D-Ser-OH	79 ± 4
25	OH	560 ± 30
26		>250
27		>500
28		>250
29		>250
30		35 ± 2
31		102 ± 5
32		26 ± 3
33		23 ± 2
34		22 ± 1
35		105 ± 14

^aIC₅₀ values were determined as the inhibitor concentration required for the half-dissociation of the complex between CBX7 and FITC-labeled H3K27me3. Data are mean values of two or three independent experimental trails. Errors reported are 95% confidence intervals.

55, 56, 59). This family of compounds revealed a broader tolerance for replacement of the backbone C=O group, such as in sulfonamide 57, which retains <10 μM potency. Interestingly, the very closely related sulfonamide 58 showed no activity, revealing a sharp dependence on the ring substituents in these compounds.

Finally, we prepared a selected set of compounds bearing multiple well-tolerated modifications to the FALKme3S scaffold (Figure 3). The competitive FP assay is convenient and accurate for moderate affinity compounds, but some of these compounds proved to be potent enough to be below the theoretical lower limit for accurate IC₅₀ measurements by competitive fluorescence polarization.^{55,56} Accordingly, we subjected the final four compounds, and also a subset of earlier compounds, to analysis by isothermal titration calorimetry (ITC) (Table 6). The ITC data indicate some degree of selectivity for CBX7 over CBX8, in spite of the 88% sequence similarity between these two chromodomains. The most potent

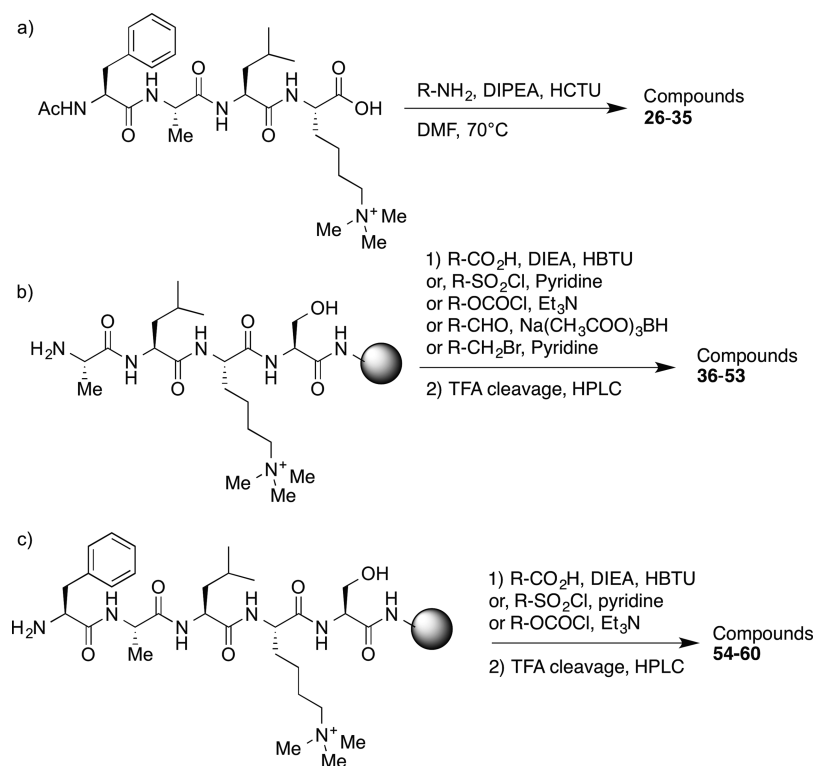
compounds against CBX7 (63 and 64) bind with $K_d \approx 200$ nM; the most selective compound (64) is ~10-fold selective over CBX8. The affinities and selectivities of the two more selective compounds most likely arise from the amide-linked aromatic ester motifs of each at their respective N-termini, which are designed to engage a region in the β-groove of CBX7/8 where significant structural divergence occurs between the two otherwise highly similar chromodomains. All other human CBX protein chromodomains are less similar to CBX7 than CBX8 (see Supporting Information), with the notable exception of CBX4. The CBX4 chromodomain is 90% similar to that of CBX7. The only two dissimilar residues in the chromodomains of these two proteins are far from the binding site, making selectivity for CBX7 over CBX4 particularly challenging. Compounds 1 and 64 showed 1.9- and 1.5-fold selectivity, respectively, for CBX7 over CBX4, and we anticipate that CBX4 will remain the most significant challenge for efforts to optimize selectivity of any CBX7 antagonists going forward. Selectivity over HP1 family chromodomains seems to be less of a problem, with initial peptide 1 having 21-fold selectivity for CBX7 over CBX1 (HP1β) and optimized compound 64 showing >2500-fold selectivity, in spite of these two chromodomains having 71% similarity scores.

The FP and ITC activity data collectively reveal a few examples of small, additive impacts of individual changes: for example, compound 54's N-terminal *p*-bromobenzamide modification improves binding by 7-fold relative to peptide 1, with further small improvements observed after inclusion of two additional substitutions at other positions (62). Elsewhere, structural features that produced differences when applied individually did not produce differences in final compounds (e.g., the two C-terminal functionalizations that create 2.5-fold differences in compounds 23 and 33 result in no difference between compounds 63 and 64). The general weakness or absence of additivities is likely due to the inherent flexibility remaining in the backbones of these peptidic compounds.

CONCLUSION

The only currently approved cancer therapies that target histone modification pathways directly are histone deacetylase inhibitors (vorinostat and romidepsin). They are relatively crude, broad spectrum drugs, but their efficacy and promise have many now creating second-generation agents (a) that are more target- and disease-specific and/or (b) that inhibit different families of molecular targets in epigenetic pathways. The numerous histone reader proteins of the human proteome offer a diverse set of functional molecular targets that appear to have great therapeutic potential. The inhibition of methyllysine reader proteins is still in its infancy, with hundreds of potential targets and therapeutic hypotheses but only a very small number of targets yet inhibited by chemical agents. The peptidic compounds reported here represent the first inhibitors of any chromodomain. While earlier inhibitors for other classes of methyllysine reader proteins have come out of high-throughput screens, we show here that generating relatively potent submicromolar peptidic leads against reader proteins is possible even when the reader protein–histone interaction on which they are initially based is relatively weak. The potential of CBX proteins as therapeutic targets will almost certainly depend on cancer and tissue type and is generally an idea that has elicited significant disagreement in the cancer biology literature. These peptidic lead compounds are intended to provide rapid access to studies of the biological effects of CBX

Scheme 1. Synthesis of (a) Compounds Bearing C-Terminal Modifications (See Table 3), (b) Analogs Bearing Phe Replacements (See Table 4), and (c) Analogs Bearing N-Terminal Additions (See Table 5)



protein antagonism, which in turn can help to test and revise therapeutic hypotheses related to chromodomain-containing proteins. We will report on these results in due course.

EXPERIMENTAL SECTION

Synthesis. Synthesis of all compounds was carried out using standard Fmoc-based solid-phase peptide synthesis protocols, modified where necessary as described in the Supporting Information. Identity and purity of all peptides were determined by HPLC–MS and were determined to be of >95% purity. Retention times reported are as determined under the following conditions: Phenomenex Luna C-18 column, 5 μm , 4.6 mm \times 250 mm, flow rate of 1 mL/min, gradient running from 90:10 water (0.1% TFA) and MeCN (0.1% TFA) to 10:90 water (0.1% TFA) and MeCN (0.1% TFA) over 30 min. Final compounds **61–64** were further characterized by ESI-MS and ^1H NMR as reported below.

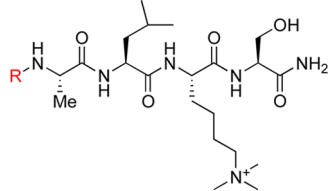
Compound 61. Compound **61** was synthesized by using manual solid phase peptide synthesis on 2-chlorotrityl resin. Coupling of the first amino acid (Fmoc-Lys(Me)₃-OH, 0.6 equiv) was done in 95:5 $\text{CH}_2\text{Cl}_2/\text{DMF}$, DIEA (2.4 equiv) as a base with stirring at ambient temperature for 2.5 h. The next two amino acid attachments were done by using standard Fmoc protocols. The N-terminal Fmoc group was deprotected upon treatment with 20% piperidine in DMF (3 \times 3 mL \times 5 min) and washed with DMF (3 \times 5 mL). This resin was treated with benzoic acid (2 equiv), HBTU (5 equiv), and DIPEA (10 equiv) for 2 h, and the resin was then washed with DMF (3 \times 5 mL) and DCM (3 \times 5 mL). The peptide was cleaved from the resin upon stirring with 1% TFA in DCM for 5 min, filtering, washing with DCM (5 \times 5 mL), and concentration in vacuo. This crude solid was then dissolved in DMF (5 mL) with HCTU (3 equiv) and DIPEA (10 equiv) and was treated with 2-amino-1,3-propanediol (3 equiv) and stirred overnight at 70 °C. Water was added (10 mL) and extracted with EtOAc (3 \times 25 mL), and the aqueous layer was evaporated to yield crude product which was then purified by HPLC as described in Supporting Information. Compound purity as determined by LC–MS: 97.63% at t_{R} = 16.21 min. LR-ESI–MS (m/z): $\text{C}_{30}\text{H}_{50}\text{N}_5\text{O}_6$, calculated

576.38, found 576.27. ^1H NMR (D_2O , 500 MHz, δ ppm) 7.46–7.35 (m, 5H), 4.37–4.32 (m, 2H), 4.09 (d, 1H, J = 10 Hz), 4.00 (quintet, 1H, J = 5 Hz), 3.73–3.62 (m, 6H), 3.36–3.25 (m, 2H), 3.10 (br s, 10H), 2.16 (sextet, 1H, J = 10 Hz), 1.93–1.70 (m, 5H), 1.69–1.51 (m, 6H), 1.48–1.33 (m, 6H), 1.3–1.18 (m, 2H).

Compound 62. Compound **62** was assembled manually on 2-chlorotrityl resin. The first amino acid was coupled as above, and the following three amino acids were attached using standard Fmoc protocols. After cleavage of Fmoc group on the N-terminus, the resin was treated with 4-bromobenzoic acid (2 equiv), HBTU (5 equiv), and DIPEA (10 equiv) for 2 h and then washed with DMF (3 \times 5 mL) and DCM (5 \times 5 mL). The peptide was cleaved from the resin by shaking with 1% TFA in DCM for 5 min, filtering, washing the resin with DCM (3 \times 5 mL), and concentration of the filtrate in vacuo. This crude peptide was taken up in DMF, and HCTU (5 equiv), DIPEA (10 equiv), and *N*-Boc-ethylenediamine were added and stirred at 70 °C overnight. The reaction mixture was diluted with water and EtOAc, the aqueous layer was extracted with EtOAc (3 \times 5 mL), and the aqueous layer was concentrated in vacuo to yield the crude compound, which was purified by HPLC as described in Supporting Information. Compound purity was determined by LC–MS, 98.72% at t_{R} = 21.52 min. LR-ESI–MS (m/z): $\text{C}_{37}\text{H}_{55}\text{N}_7\text{O}_5$, calculated 756.34/758.34, found 756.34/758.34. ^1H NMR (D_2O , 300 MHz, δ ppm), 7.6 (d, 2H, J = 9 Hz), 7.5 (d, 2H, J = 9 Hz), 4.26–4.16 (m, 1H), 3.96 (d, 2H, J = 12 Hz), 3.52–3.33 (m, 2H), 3.18 (q, 3H, J = 9 Hz), 3.07–3.01 (m, 3H), 2.98 (br s, 10H), 1.80–1.61 (m, 4H), 1.60–1.08 (m, 12H).

Compound 63. The peptide FA(cyclopropyl-Gly)Kme₅(D-S) was synthesized on Rink amide resin using CEM Liberty microwave synthesizer standard Fmoc protocols. The N-terminal deprotected peptide, on resin, was treated with monomethyl terephthalate (5 equiv) that was preactivated by shaking with HBTU (5 equiv) and DIPEA (10 equiv) in DMF for 2 min. This solution was added to the resin and allowed to stir at ambient temperature overnight. The solution was filtered and resin washed with DMF (3 \times 5 mL) and DCM (3 \times 5 mL) and air-dried. The peptide was cleaved from resin upon treatment with 10 mL 95:2.5:2.5 TFA/ H_2O /triisopropylsilane for 2 h. This solution was then concentrated in vacuo and upon

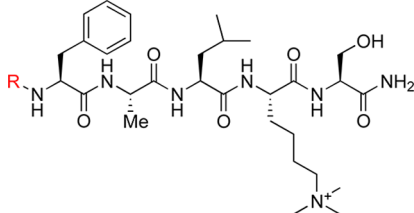
Table 4. H3K27me3-CBX7 Disruption by FALKme3S Analogs Bearing Phe (-3) Replacements



Compound	R =	IC ₅₀ (μM) ^a
1	Ac-Phe	11 ± 0.4
36	Ac-Tyr	8.6 ± 0.5
37	Ac-Trp	7.8 ± 0.5
38	Ac-Phg	26 ± 1
39		57 ± 3
40		91 ± 19
41		23 ± 1
42		89 ± 14
43		26 ± 1
44		67 ± 6
45		58 ± 7.1
46		100 ± 15
47		58 ± 6
48		>250
49		>250
50		34 ± 1
51		53 ± 2
52		>2mM
53		>2mM

^aIC₅₀ values were determined as the inhibitor concentration required for the half-dissociation of the complex between CBX7 and FITC-labeled H3K27me3. Data are mean values of two or three independent experimental trails. Errors reported are 95% confidence intervals.

Table 5. H3K27me3-CBX7 Disruption by FALKme3S Analogs Bearing Phe (-3) Replacements



Compound	R =	IC ₅₀ (μM) ^a
1	Ac	11 ± 0.4
54		4.6 ± 0.3
55		6.2 ± 0.2
56		6.3 ± 0.4
57		6.7 ± 0.4
58		>250
59		8.8 ± 0.5
60		57 ± 9

^aIC₅₀ values were determined as the inhibitor concentration required for the half-dissociation of the complex between CBX7 and FITC-labeled H3K27me3. Data are mean values of two or three independent experimental trails. Errors reported are 95% confidence intervals.

treatment with cold diethyl ether yielded crude white precipitate which was collected by centrifugation. This crude product was then purified by HPLC (see Supporting Information). Compound purity determined by LC-MS, purity >99% at *t_R* = 20.8 min. LR-ESI-MS (*m/z*): C₄₀H₅₈N₇O₉⁺ calculated 780.4, found 780.0. ¹H NMR (D₂O, 500 MHz, δ ppm) 8.09 (br d, 2H), 7.76 (br d, 2H), 7.36 (m, 5H), 4.38 (m, 3H), 4.08 (br d, 1H), 3.96 (s, 2H), 3.89 (m, 3H), 3.31 (m, 3H), 3.09 (s, 9H), 2.19 (m, 1H), 1.65 (m, 13H), 1.35 (d, 7.4 Hz, 3H), 1.25 (m, 2H).

Compound 64. Peptide FA(cyclopropyl-Gly)Kme₃ was first synthesized on 2-chlorotrityl resin. Coupling of the first amino acid (Fmoc-Lys(Me)₃-OH, 0.6 equiv) was done in 95:5 CH₂Cl₂/DMF, DIEA (2.4 equiv) as a base and stirred at ambient temperature for 2.5 h. Further amino acids attachments, deprotection, and acetylation on the N-terminus were performed as above. The N-terminal Fmoc group was deprotected upon treatment with 20% piperidine in DMF (3 × 3 mL × 5 min). While the peptide was still on resin, monomethyl terephthalate (5 equiv) was preactivated by shaking with HBTU (5 equiv) and DIPEA (10 equiv) in DMF for 2 min. This solution was added to the resin and allowed to stir at ambient temperature overnight. The solution was filtered and resin washed with DMF (3 × 5 mL) and DCM (3 × 5 mL) and air-dried. The peptide was cleaved from resin upon treatment with 10 mL of 95:2.5:2.5 TFA/H₂O/triisopropylsilane for 2 h. This solution was then concentrated in vacuo and upon treatment with cold diethyl ether yielded crude white precipitate that was collected by centrifugation. This crude solid was then dissolved in DMF (5 mL) with HCTU (3 equiv) and DIPEA (10

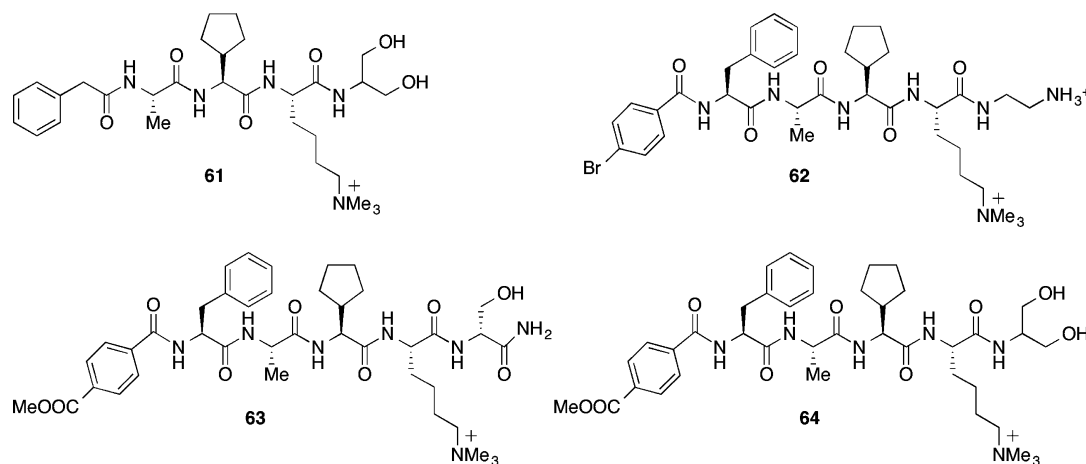


Figure 3. Final set of peptidic CBX7 inhibitors bearing multiple functional group replacements.

Table 6. K_d Values (μM) Arising from ITC Titration of Selected Compounds into Chromodomains of CBX7, CBX8, CBX4, and CBX1^a

compd	CBX7	CBX8	CBX4	CBX1
1	2.00 ± 0.20	14.2 ± 2.0	3.7 ± 0.5	43 ± 2.8
11	1.77 ± 0.12	12.3 ± 1.4	nd	nd
23	5.4 ± 0.9	15.0 ± 2.8	nd	nd
54	0.28 ± 0.05	1.5 ± 0.3	nd	nd
61	4.1 ± 0.2	15.0 ± 3.0	nd	nd
62	0.22 ± 0.02	0.48 ± 0.04	nd	nd
63	0.20 ± 0.03	1.78 ± 0.25	nd	nd
64	0.20 ± 0.04	1.89 ± 0.16	0.29 ± 0.02	>500

^aAveraged values determined by duplicate ITC titrations at 298 K in buffered H₂O (20 mM Tris, 250 mM NaCl, 1 mM DTT, pH 8). See Supporting Information for experimental details, thermodynamic parameters, and exemplary raw data.

equiv) and was treated with 2-amino-1,3-propanediol (3 equiv) and stirred overnight at room temperature. Water was added (10 mL) and extracted with ethyl acetate (3 × 25 mL), and the aqueous layer was evaporated to yield crude product, which was purified by HPLC (see Supporting Information). Compound purity determined by LC–MS >99% at $t_R = 21.0$ min. LR-ESI-MS (m/z): C₄₀H₅₉N₆O₉⁺ calculated 767.4, found 767.9. ¹H NMR (D₂O, 500 MHz, δ ppm), 8.1 (d, 7.8 Hz, 2H), 7.77 (d, 7.8 Hz, 2H), 7.35 (m, 5H), 4.34 (m, 2H), 4.05 (d, 7.9 Hz, 1H), 3.96 (s + underlying m, 4H), 3.31 (m, 3H), 3.18 (m, 1H), 3.09 (s + s, 9H), 2.18 (q, 8 Hz, 9 Hz, 1H), 1.70 (m, 12H), 1.35 (d, 6.4 Hz, 3H), 1.25 (m, 2H).

Protein Expression and Fluorescence Polarization Assay for CBX7-H3K27me3 Disruption. Chromodomains were expressed and purified as previously reported,³¹ using Addgene plasmids 25241 (CBX7), 25245 (CBX1), and 25237 (CBX4) deposited by C. Arrowsmith, Structural Genomics Consortium, Toronto, Canada, and an analogous plasmid for CBX8 generously donated directly to us by C. Arrowsmith. The conditions for competitive FP assay were adapted from those used in an earlier report of a direct protein-into-peptide titration.³¹ The peptide FITC-H3K27me₃, BSA, and inhibitors were resuspended in distilled H₂O. The assay was performed in black, 96-well plates (NUNC) in a buffer containing 20 mM Tris-HCl, pH 8.0, 250 mM NaCl, 1 mM DTT, 1 mM benzamidine, 1 mM PMSEF, 0.01% Tween. Constant concentrations of CBX7 and FITC-K27me₃ were 8.68 μM and 500 nM, respectively. Inhibitor concentrations varied from 0 to 2 mM, and all wells were made up to a final volume of 100 μL . Plates were incubated for 15 min in darkness prior to reading with a SpectraMax M5 plate reader (Molecular Devices) with $\lambda_{\text{exc}} = 450$ nm, $\lambda_{\text{obs}} = 530$ nm, and an instrument cutoff of 515 nm. The parallel and perpendicular intensities of emission were adjusted for

background of the blank buffer, giving millipolarization (mP) values for each reading that were determined and normalized to percentage of complex formed. Values were graphed using XLfit (IDBS) and fitted using a sigmoidal curve function from which IC₅₀ values were extrapolated and standard error was derived. Experiments were performed in triplicate, and the IC₅₀ values reported are the averages of all values.

Isothermal Titration Calorimetry. Isothermal titration calorimetry was carried out on a VP-ITC (Microcal, Inc.) at 298 K in Tris-buffered water (20 mM Tris, 250 mM NaCl, 1 mM DTT, pH 8). Inhibitor concentration in the syringe was 0.75–1.0 mM, which was titrated into a sample in matched buffer of protein at a concentration of 50–70 μM . After subtraction of background heats of dilution, curve fitting was carried out using “one-set-of-sites” binding model of the manufacturer’s supplied Origin software. See Supporting Information for raw and fitted data.

■ ASSOCIATED CONTENT

Supporting Information

Supplementary experimental procedures for peptide synthesis; ¹H NMR spectra for compounds 61–64; experimental procedures and supplementary figures for X-ray crystallography and 2D-NMR studies; chromodomain sequences, alignments, and structural comparisons; raw and fitted ITC data. This material is available free of charge via the Internet at <http://pubs.acs.org>.

Accession Codes

The coordinates of the complex between CBX7 and ligand 11 have been deposited in the Protein Data Bank (PDB code 4MN3).

■ AUTHOR INFORMATION

Corresponding Author

*Phone: 1-250-721-7193. E-mail: fhof@uvic.ca.

Author Contributions

[†]C.S. and K.D.D. contributed equally to this work.

Notes

The authors declare no competing financial interest.

■ ACKNOWLEDGMENTS

This work was supported by the West Coast Ride to Live Grants for Prostate Cancer Research and a Grant from Prostate Cancer Canada. K.D.D. acknowledges fellowship support from the West Coast Ride to Live—Vancouver Island and from the Prostate Cancer Foundation of British Columbia. M.J.B.,

J.E.W., and F.H. are Scholars of the Michael Smith Foundation for Health Research and Canada Research Chairs. We thank O. Granot and C. Barr for expert assistance with MS and NMR instrumentation and experiments. We thank C. Arrowsmith, Structural Genomics Consortium Toronto, for contributing the chromodomain plasmids.

■ ABBREVIATIONS USED

Abu, 2-aminobutyric acid; BSA, bovine serum albumin; CBX, chromobox homolog; DCM, dichloromethane; DIPEA, ethyl-diisopropylamine; EZH2, enhancer of zeste homolog 2; FP, fluorescence polarization; H3K27me3, histone 3, lysine 27 trimethylated; HBTU, 1*H*-benzotriazol-1-yl[bis-(dimethylamino)methylene]oxonium hexafluorophosphate; HCTU, [(6-chloro-1*H*-benzotriazol-1-yl)oxy]-(dimethylamino)-*N,N*-dimethyliminium hexafluorophosphate; ITC, isothermal titration calorimetry; Nle, norleucine; 3-PAL, 3-pyridylalanine; Phg, phenylglycine; PRC1/2, polycomb repressive complex 1/2; SETDB1, histone-lysine *N*-methyltransferase SETDB1 (KMT1E)

■ REFERENCES

- (1) Strahl, B. D.; Allis, C. D. The language of covalent histone modifications. *Nature* **2000**, *403*, 41–45.
- (2) de la Cruz, X.; Lois, S.; Sanchez-Molina, S.; Martinez-Balbas, M. A. Do protein motifs read the histone code? *BioEssays* **2005**, *27*, 164–175.
- (3) Migliori, V.; Muller, J.; Phalke, S.; Low, D.; Bezzi, M.; Mok, W. C.; Sahu, S. K.; Gunaratne, J.; Capasso, P.; Bassi, C.; Cecatiello, V.; De Marco, A.; Blackstock, W.; Kuznetsov, V.; Amati, B.; Mapelli, M.; Guccione, E. Symmetric dimethylation of H3R2 is a newly identified histone mark that supports euchromatin maintenance. *Nat. Struct. Mol. Biol.* **2012**, *19*, 136–144.
- (4) Taverna, S. D.; Li, H.; Ruthenburg, A. J.; Allis, C. D.; Patel, D. J. How chromatin-binding modules interpret histone modifications: lessons from professional pocket pickers. *Nat. Struct. Mol. Biol.* **2007**, *14*, 1025–1040.
- (5) Daigle, S. R.; Olhava, E. J.; Therkelsen, C. A.; Basavapathruni, A.; Jin, L.; Boriack-Sjodin, P. A.; Allain, C. J.; Klaus, C. R.; Raimondi, A.; Scott, M. P.; Waters, N. J.; Chesworth, R.; Moyer, M. P.; Copeland, R. A.; Richon, V. M.; Pollock, R. M. Potent inhibition of DOT1L as treatment of MLL-fusion leukemia. *Blood* **2013**, *122*, 1017–1025.
- (6) Anglin, J. L.; Song, Y. A medicinal chemistry perspective for targeting histone H3 lysine-79 methyltransferase DOT1L. *J. Med. Chem.* **2013**, *56*, 8972–8983.
- (7) Takawa, M.; Masuda, K.; Kunizaki, M.; Daigo, Y.; Takagi, K.; Iwai, Y.; Cho, H.-S.; Toyokawa, G.; Yamane, Y.; Maejima, K.; Field, H. I.; Kobayashi, T.; Akasu, T.; Sugiyama, M.; Tsuchiya, E.; Atomi, Y.; Ponder, B. A. J.; Nakamura, Y.; Hamamoto, R. Validation of the histone methyltransferase EZH2 as a therapeutic target for various types of human cancer and as a prognostic marker. *Cancer Sci.* **2011**, *102*, 1298–1305.
- (8) McCabe, M. T.; Ott, H. M.; Ganji, G.; Korenchuk, S.; Thompson, C.; Van Aller, G. S.; Liu, Y.; Graves, A. P.; Della Pietra, A., 3rd; Diaz, E.; LaFrance, L. V.; Mellinger, M.; Duquenne, C.; Tian, X.; Kruger, R. G.; McHugh, C. F.; Brandt, M.; Miller, W. H.; Dhanak, D.; Verma, S. K.; Tummino, P. J.; Creasy, C. L. EZH2 inhibition as a therapeutic strategy for lymphoma with EZH2-activating mutations. *Nature* **2012**, *492*, 108–112.
- (9) Verma, S. K.; Tian, X. R.; LaFrance, L. V.; Duquenne, C.; Suarez, D. P.; Newlander, K. A.; Romeril, S. P.; Burgess, J. L.; Grant, S. W.; Brackley, J. A.; Graves, A. P.; Scherzer, D. A.; Shu, A.; Thompson, C.; Ott, H. M.; Van Aller, G. S.; Machutta, C. A.; Diaz, E.; Jiang, Y.; Johnson, N. W.; Knight, S. D.; Kruger, R. G.; McCabe, M. T.; Dhanak, D.; Tummino, P. J.; Creasy, C. L.; Miller, W. H. Identification of potent, selective, cell-active inhibitors of the histone lysine methyltransferase EZH2. *ACS Med. Chem. Lett.* **2012**, *3*, 1091–1096.
- (10) Knutson, S. K.; Warholik, N. M.; Wigle, T. J.; Klaus, C. R.; Allain, C. J.; Raimondi, A.; Porter Scott, M.; Chesworth, R.; Moyer, M. P.; Copeland, R. A.; Richon, V. M.; Pollock, R. M.; Kuntz, K. W.; Keilhack, H. Durable tumor regression in genetically altered malignant rhabdoid tumors by inhibition of methyltransferase EZH2. *Proc. Natl. Acad. Sci. U.S.A.* **2013**, *110*, 7922–7927.
- (11) Wigle, T. J.; Copeland, R. A. Drugging the human methylome: an emerging modality for reversible control of aberrant gene transcription. *Curr. Opin. Chem. Biol.* **2013**, *17*, 369–378.
- (12) Yao, Y.; Chen, P.; Diao, J.; Cheng, G.; Deng, L.; Anglin, J. L.; Prasad, B. V.; Song, Y. Selective inhibitors of histone methyltransferase DOT1L: design, synthesis, and crystallographic studies. *J. Am. Chem. Soc.* **2011**, *133*, 16746–16749.
- (13) Marks, P. A. Discovery and development of SAHA as an anticancer agent. *Oncogene* **2007**, *26*, 1351–1356.
- (14) Stimson, L.; Wood, V.; Khan, O.; Fotheringham, S.; La Thangue, N. B. HDAC inhibitor-based therapies and haematological malignancy. *Ann. Oncol.* **2009**, *20*, 1293–1302.
- (15) New, M.; Olzscha, H.; La Thangue, N. B. HDAC inhibitor-based therapies: Can we interpret the code? *Mol. Oncol.* **2012**, *6*, 637–656.
- (16) Matzuk, M. M.; McKeown, M. R.; Filippakopoulos, P.; Li, Q.; Ma, L.; Agno, J. E.; Lemieux, M. E.; Picaud, S.; Yu, R. N.; Qi, J.; Knapp, S.; Bradner, J. E. Small-molecule inhibition of BRDT for male contraception. *Cell* **2012**, *150*, 673–684.
- (17) Banerjee, C.; Archin, N.; Michaels, D.; Belkina, A. C.; Denis, G. V.; Bradner, J.; Sebastiani, P.; Margolis, D. M.; Montano, M. BET bromodomain inhibition as a novel strategy for reactivation of HIV-1. *J. Leukocyte Biol.* **2012**, *92*, 1147–1154.
- (18) Filippakopoulos, P.; Qi, J.; Picaud, S.; Shen, Y.; Smith, W. B.; Fedorov, O.; Morse, E. M.; Keates, T.; Hickman, T. T.; Feltetar, I.; Philpott, M.; Munro, S.; McKeown, M. R.; Wang, Y.; Christie, A. L.; West, N.; Cameron, M. J.; Schwartz, B.; Heightman, T. D.; La Thangue, N.; French, C. A.; Wiest, O.; Kung, A. L.; Knapp, S.; Bradner, J. E. Selective inhibition of BET bromodomains. *Nature* **2010**, *468*, 1067–1073.
- (19) Loven, J.; Hoke, H. A.; Lin, C. Y.; Lau, A.; Orlando, D. A.; Vakoc, C. R.; Bradner, J. E.; Lee, T. I.; Young, R. A. Selective inhibition of tumor oncogenes by disruption of super-enhancers. *Cell* **2013**, *153*, 320–334.
- (20) Liu, L.; Zhen, X. T.; Denton, E.; Marsden, B. D.; Schapira, M. ChromoHub: a data hub for navigators of chromatin-mediated signalling. *Bioinformatics* **2012**, *28*, 2205–2206.
- (21) Yap, K. L.; Zhou, M. M. Structure and mechanisms of lysine methylation recognition by the chromodomain in gene transcription. *Biochemistry* **2011**, *50*, 1966–1980.
- (22) Santiago, C.; Nguyen, K.; Schapira, M. Druggability of methyl-lysine binding sites. *J. Comput.-Aided. Mol. Des.* **2011**, *25*, 1171–1178.
- (23) Kireev, D.; Wigle, T. J.; Norris-Drouin, J.; Herold, J. M.; Janzen, W. P.; Frye, S. V. Identification of non-peptide malignant brain tumor (MBT) repeat antagonists by virtual screening of commercially available compounds. *J. Med. Chem.* **2010**, *53*, 7625–7631.
- (24) Gao, C.; Herold, J. M.; Kireev, D.; Wigle, T.; Norris, J. L.; Frye, S. Biophysical probes reveal a “compromise” nature of the methyl-lysine binding pocket in L3MBTL1. *J. Am. Chem. Soc.* **2011**, *133*, 5357–5362.
- (25) Herold, J. M.; Wigle, T. J.; Norris, J. L.; Lam, R.; Korboukh, V. K.; Gao, C.; Ingerman, L. A.; Kireev, D. B.; Senisterra, G.; Vedadi, M.; Tripathy, A.; Brown, P. J.; Arrowsmith, C. H.; Jin, J.; Janzen, W. P.; Frye, S. V. Small-molecule ligands of methyl-lysine binding proteins. *J. Med. Chem.* **2011**, *54*, 2504–2511.
- (26) James, L. I.; Korboukh, V. K.; Krichevsky, L.; Baughman, B. M.; Herold, J. M.; Norris, J. L.; Jin, J.; Kireev, D. B.; Janzen, W. P.; Arrowsmith, C. H.; Frye, S. V. Small-molecule ligands of methyl-lysine binding proteins: optimization of selectivity for L3MBTL3. *J. Med. Chem.* **2013**, *56*, 7358–7371.
- (27) Camerino, M. A.; Zhong, N.; Dong, A.; Dickson, B.; James, L.; Baughman, B.; Norris, J.; Kireev, D.; Janzen, W. P.; Arrowsmith, C.; Frye, S. V. The structure–activity relationships of L3MBTL3

inhibitors: a second series of potent compounds which bind the L3MBTL3 dimer. *MedChemComm* **2013**, *4*, 1501–1507.

(28) James, L. I.; Barysyt-Lovejoy, D.; Zhong, N.; Krichevsky, L.; Korboukh, V. K.; Herold, J. M.; MacNevin, C. J.; Norris, J. L.; Sagum, C. A.; Tempel, W.; Marcon, E.; Guo, H. B.; Gao, C.; Huang, X. P.; Duan, S. L.; Emili, A.; Greenblatt, J. F.; Kireev, D. B.; Jin, J.; Janzen, W. P.; Brown, P. J.; Bedford, M. T.; Arrowsmith, C. H.; Frye, S. V. Discovery of a chemical probe for the L3MBTL3 methyllysine reader domain. *Nat. Chem. Biol.* **2013**, *9*, 184–191.

(29) Wagner, E. K.; Nath, N.; Flemming, R.; Feltenberger, J. B.; Denu, J. M. Identification and characterization of small molecule inhibitors of a plant homeodomain finger. *Biochemistry* **2012**, *51*, 8293–8306.

(30) Eissenberg, J. C. Structural biology of the chromodomain: form and function. *Gene* **2012**, *496*, 69–78.

(31) Kaustov, L.; Ouyang, H.; Amaya, M.; Lemak, A.; Nady, N.; Duan, S.; Wasney, G. A.; Li, Z.; Vedadi, M.; Schapira, M.; Min, J.; Arrowsmith, C. H. Recognition and specificity determinants of the human cbx chromodomains. *J. Biol. Chem.* **2011**, *286*, 521–529.

(32) Blus, B. J.; Wiggins, K.; Khorasanizadeh, S. Epigenetic virtues of chromodomains. *Crit. Rev. Biochem. Mol. Biol.* **2011**, *46*, 507–526.

(33) Gieni, R. S.; Hendzel, M. J. Polycomb group protein gene silencing, non-coding RNA, stem cells, and cancer. *Biochem. Cell Biol.* **2009**, *87*, 711–746.

(34) Bracken, A. P.; Helin, K. Polycomb group proteins: navigators of lineage pathways led astray in cancer. *Nat. Rev. Cancer* **2009**, *9*, 773–784.

(35) Sauvageau, M.; Sauvageau, G. Polycomb group proteins: multifaceted regulators of somatic stem cells and cancer. *Cell Stem Cell* **2010**, *7*, 299–313.

(36) Morey, L.; Pascual, G.; Cozzuto, L.; Roma, G.; Wutz, A.; Benitah, S. A.; Di Croce, L. Nonoverlapping functions of the Polycomb group Cbx family of proteins in embryonic stem cells. *Cell Stem Cell* **2012**, *10*, 47–62.

(37) O'Loughlen, A.; Munoz-Cabello, A. M.; Gaspar-Maia, A.; Wu, H. A.; Banito, A.; Kunowska, N.; Racek, T.; Pemberton, H. N.; Beolchi, P.; Lavial, F.; Masui, O.; Vermeulen, M.; Carroll, T.; Graumann, J.; Heard, E.; Dillon, N.; Azuara, V.; Snijders, A. P.; Peters, G.; Bernstein, E.; Gil, J. MicroRNA regulation of Cbx7 mediates a switch of Polycomb orthologs during ESC differentiation. *Cell Stem Cell* **2012**, *10*, 33–46.

(38) Gil, J.; Bernard, D.; Martinez, D.; Beach, D. Polycomb CBX7 has a unifying role in cellular lifespan. *Nat. Cell Biol.* **2004**, *6*, 67–72.

(39) Bernard, D.; Martinez-Leal, J. F.; Rizzo, S.; Martinez, D.; Hudson, D.; Visakorpi, T.; Peters, G.; Carnero, A.; Beach, D.; Gil, J. CBX7 controls the growth of normal and tumor-derived prostate cells by repressing the Ink4a/Arf locus. *Oncogene* **2005**, *24*, 5543–5551.

(40) Yap, K. L.; Li, S.; Muñoz-Cabello, A. M.; Raguz, S.; Zeng, L.; Mujtaba, S.; Gil, J.; Walsh, M. J.; Zhou, M.-M. Molecular interplay of the noncoding RNA ANRIL and methylated histone H3 lysine 27 by Polycomb CBX7 in transcriptional silencing of INK4a. *Mol. Cell* **2010**, *38*, 662–674.

(41) NCT01897571 information available on <http://www.clinicaltrials.gov>.

(42) van den Boom, V.; Rozenveld-Geugien, M.; Bonardi, F.; Malanga, D.; van Gosliga, D.; Heijink, A. M.; Viglietto, G.; Morrone, G.; Fusetti, F.; Vellenga, E.; Schuringa, J. J. Non-redundant and locus-specific gene repression functions of PRC1 paralog family members in human hematopoietic stem/progenitor cells. *Blood* **2013**, *121*, 2452–2461.

(43) Scott, C. L.; Gil, J.; Hernando, E.; Teruya-Feldstein, J.; Narita, M.; Martinez, D.; Visakorpi, T.; Mu, D.; Cordon-Cardo, C.; Peters, G.; Beach, D.; Lowe, S. W. Role of the chromobox protein CBX7 in lymphomagenesis. *Proc. Natl. Acad. Sci. U.S.A.* **2007**, *104*, 5389–5394.

(44) Shinjo, K.; Yamashita, Y.; Yamamoto, E.; Akatsuka, S.; Uno, N.; Kamiya, A.; Niimi, K.; Sakaguchi, Y.; Nagasaka, T.; Takahashi, T.; Shibata, K.; Kajiyama, H.; Kikkawa, F.; Toyokuni, S. Expression of chromobox homolog 7 (CBX7) is associated with poor prognosis in ovarian clear cell adenocarcinoma via TRAIL-induced apoptotic

pathway regulation. *Int. J. Cancer* [Online early access]. DOI: 10.1002/ijc.28692. Published Online: Jan 10, 2014.

(45) Wyatt, A.; Collins, C. Vancouver Prostate Centre, personal communication.

(46) Klauke, K.; Radulovic, V.; Broekhuis, M.; Weersing, E.; Zwart, E.; Olthof, S.; Ritsema, M.; Bruggeman, S.; Wu, X.; Helin, K.; Bystrykh, L.; de Haan, G. Polycomb Cbx family members mediate the balance between haematopoietic stem cell self-renewal and differentiation. *Nat. Cell Biol.* **2013**, *15*, 353–362.

(47) Perry, A. S. Prostate cancer epigenomics. *J. Urol.* **2013**, *189*, 10–11.

(48) Pallante, P.; Terracciano, L.; Carafa, V.; Schneider, S.; Zlobec, I.; Lugli, A.; Bianco, M.; Ferraro, A.; Sacchetti, S.; Troncone, G.; Fusco, A.; Tornillo, L. The loss of the CBX7 gene expression represents an adverse prognostic marker for survival of colon carcinoma patients. *Eur. J. Cancer* **2010**, *46*, 2304–2313.

(49) Pallante, P.; Federico, A.; Berlingieri, M. T.; Bianco, M.; Ferraro, A.; Forzati, F.; Iaccarino, A.; Russo, M.; Pierantoni, G. M.; Leone, V.; Sacchetti, S.; Troncone, G.; Santoro, M.; Fusco, A. Loss of the CBX7 gene expression correlates with a highly malignant phenotype in thyroid cancer. *Cancer Res.* **2008**, *68*, 6770–6778.

(50) Federico, A.; Pallante, P.; Bianco, M.; Ferraro, A.; Esposito, F.; Monti, M.; Cozzolino, M.; Keller, S.; Fedele, M.; Leone, V.; Troncone, G.; Chiariotti, L.; Pucci, P.; Fusco, A. Chromobox protein homologue 7 protein, with decreased expression in human carcinomas, positively regulates E-cadherin expression by interacting with the histone deacetylase 2 protein. *Cancer Res.* **2009**, *69*, 7079–7087.

(51) Forzati, F.; Federico, A.; Pallante, P.; Abbate, A.; Esposito, F.; Malapelle, U.; Sepe, R.; Palma, G.; Troncone, G.; Scarfo, M.; Arra, C.; Fedele, M.; Fusco, A. CBX7 is a tumor suppressor in mice and humans. *J. Clin. Invest.* **2012**, *122*, 612–623.

(52) Klauke, K.; Radulović, V.; Broekhuis, M.; Weersing, E.; Zwart, E.; Olthof, S.; Ritsema, M.; Bruggeman, S.; Wu, X.; Helin, K.; Bystrykh, L.; de Haan, G. Polycomb Cbx family members mediate the balance between haematopoietic stem cell self-renewal and differentiation. *Nat. Cell Biol.* **2013**, *15*, 353–362.

(53) qHTS Validation Assay for Inhibitors of HP1-beta Chromodomain Interactions with Methylated Histone Tails. <http://pubchem.ncbi.nlm.nih.gov/assay/assay.cgi?aid=488953>.

(54) Completing the coordination of the Mg²⁺ are a symmetry related Glu/His pair from another monomer. This suggests indirectly that multimerization, either with another copy of CBX7 or with another member of the PRC1 complex, might play a role in stabilizing the bound metal in vivo.

(55) Huang, X. Fluorescence polarization competition assay: the range of resolvable inhibitor potency is limited by the affinity of the fluorescent ligand. *J. Biomol. Screening* **2003**, *8*, 34–38.

(56) The lower limit for any IC₅₀ determined by competitive fluorescence polarization assay is approximately the K_d value for the dissociation of probe peptide from protein target. This value for CBX7 and the H3K27me3 probe peptide is 7 μM under our experimental conditions, and so compounds with greater potency than K_d ≈ 7 μM generate IC₅₀ values that are only marginally lower than this regardless of how potent they are (see ref 55 for a detailed explanation). Direct comparison of IC₅₀ values determined by competitive FP and K_d values determined by ITC confirms the existence of the lower limit for competitive FP measurements. For example, compound 54 has an IC₅₀ value measured at 4.6 μM by competitive FP but is shown to have a true K_d of 280 nM when measured by ITC.